2.4.4 Results for Asymmetric Bar

For verification of the dynamic equations developed and the program written for the asymmetric case, they were again checked for the symmetric case a = 0. The resulting transmissibility values and peak frequencies were the same as those presented in Section 2.3.3.

Transmissibility versus frequency plots were then generated for various values of b_1. By keeping the rest of the parameters at constant values, the effect of the changing center of mass can be studied by comparing the plots and their peak frequencies. The values of the parameters that are kept constant throughout this chapter are as follows: h=0.1, b=0.5, p_o=40, c=1, and r=1.

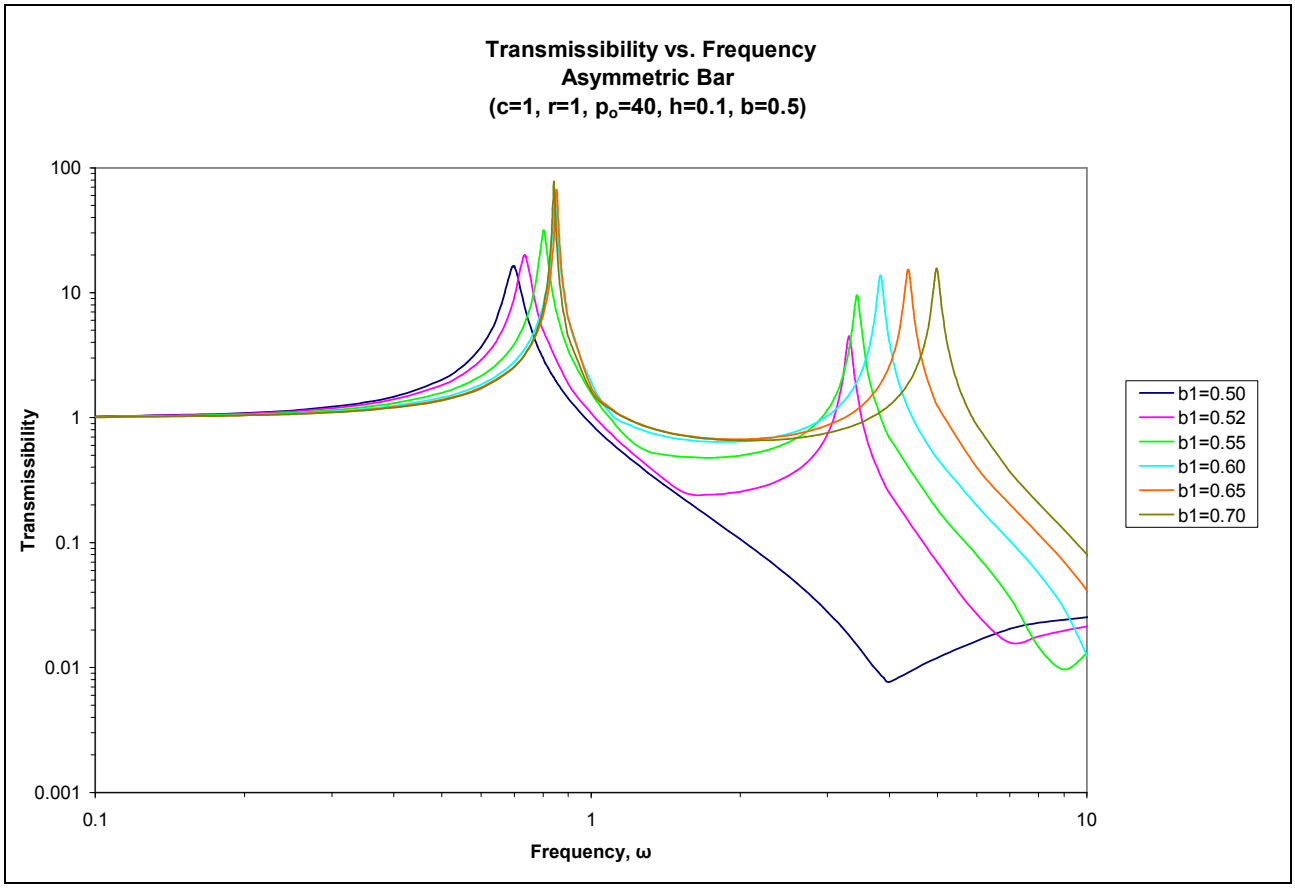

Figure 2.17 Transmissibility vs. Frequency for Different Values of b_1

Figure 2.17 shows the first two frequency peaks for values of $b_1 = 0.50$ (symmetric case), 0.52, 0.55, 0.60, 0.65, and 0.70. The most notable difference between all of the asymmetric cases and the symmetric case is that the symmetric case has no second peak at a value of ω in the range of three to five. It can also be seen that as the asymmetry of the bar increases, the peak frequencies increase.

To further examine the effects of different degrees of asymmetry, transmissibility values were determined for each value of b_1 shown in Figure 2.17 up to a frequency $\omega = 200$, and some vibration shapes at various frequencies were determined as well. Figures 2.18, 2.19, and 2.20 show transmissibility vs. frequency plots and vibration shapes for values of b_1 equal to 0.52, 0.60, and 0.70, respectively. Transmissibility vs. frequency plots for b_1 equal to 0.55 and 0.65 can be seen in Appendix E.

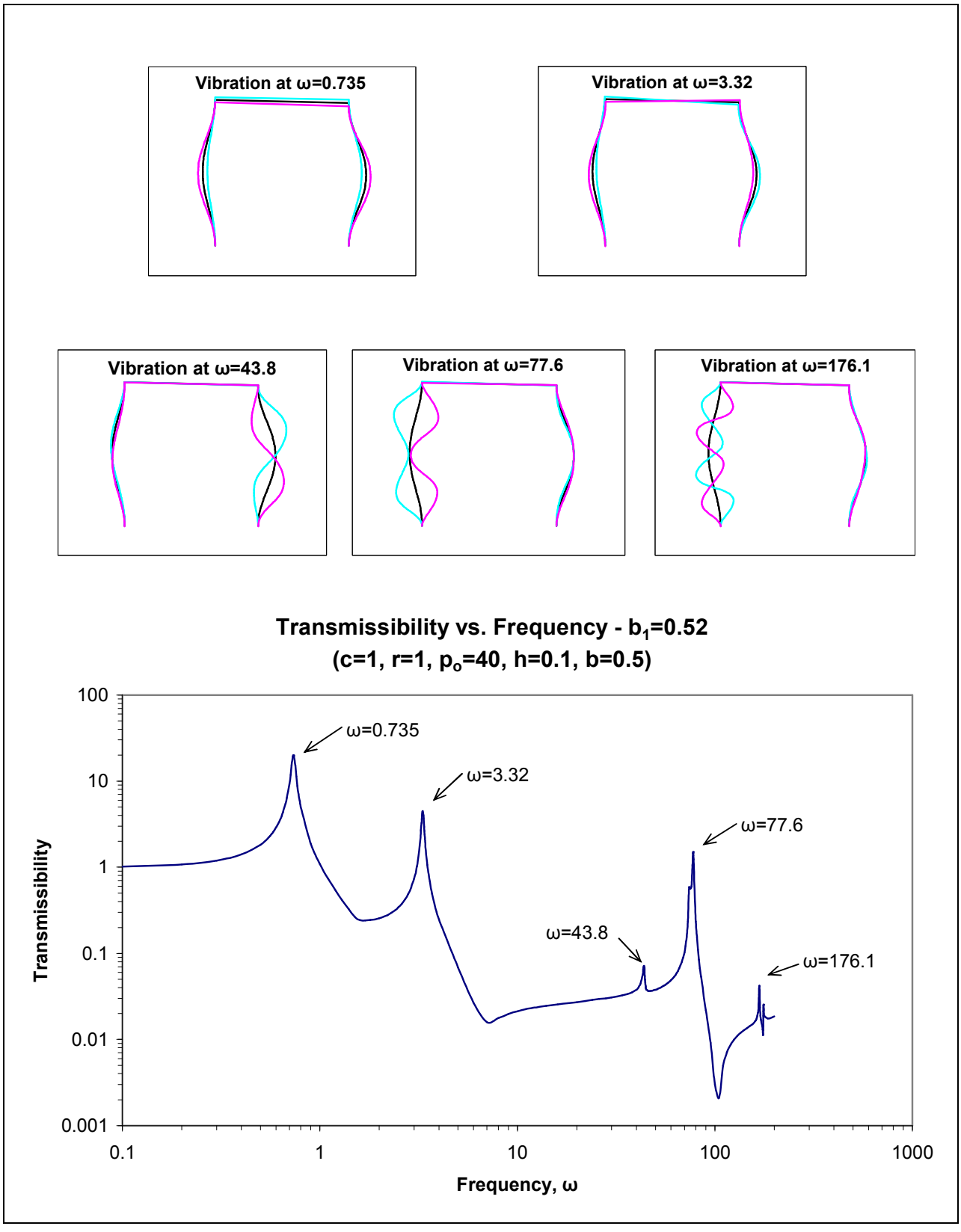

Figure 2.18 Transmissibility vs. Frequency and Vibration Shapes for $b_1 = 0.52$

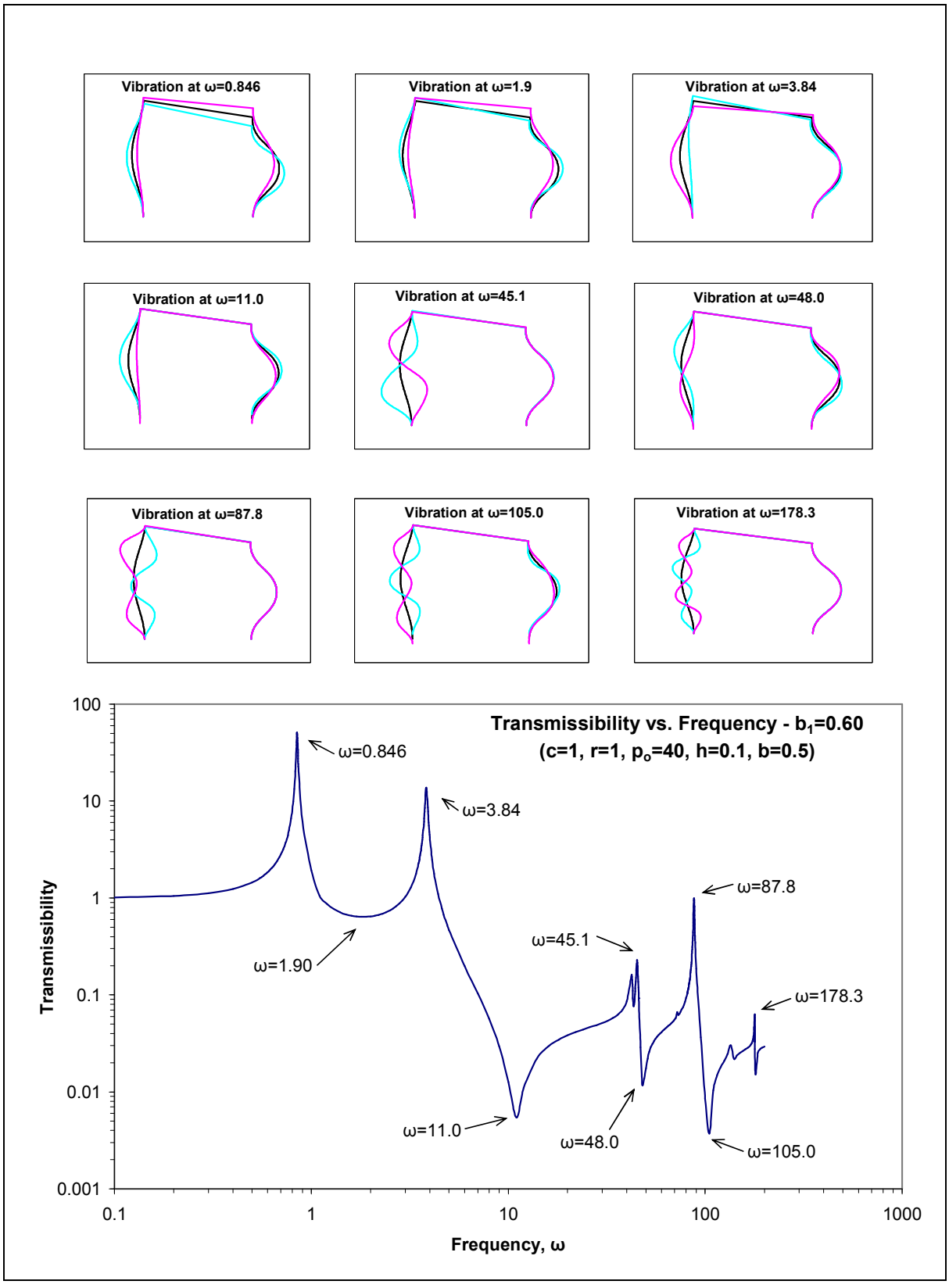

Figure 2.19 Transmissibility vs. Frequency and Vibration Shapes for $b_1 = 0.60$

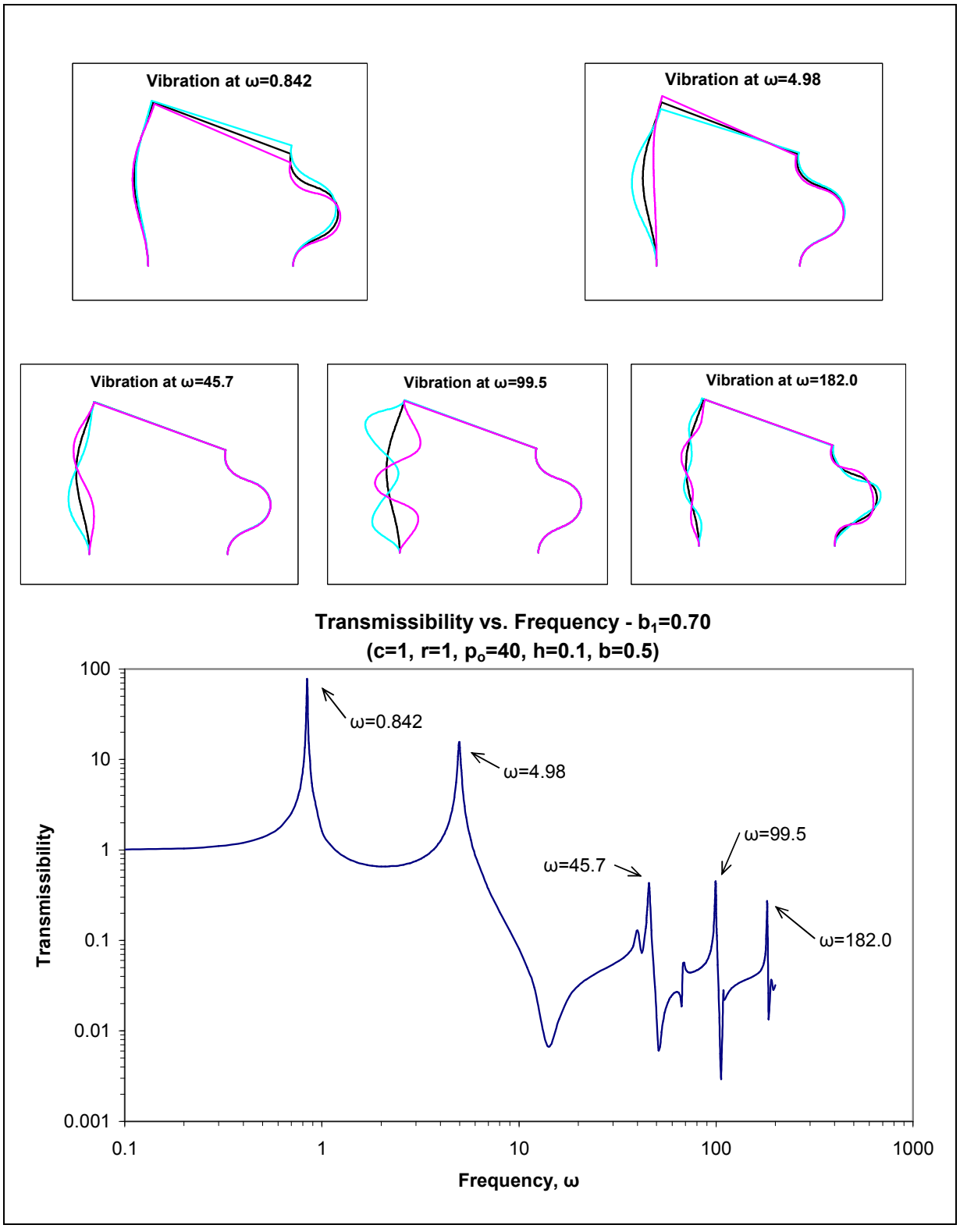

Figure 2.20 Transmissibility vs. Frequency and Vibration Shapes for $b_1 = 0.70$

When observing the transmissibility plots in Figures 2.18-2.20, they look quite similar. They each have five significant frequency peaks, and they each have a range of frequency from about 3 to 70 in which the transmissibility is well below unity. As observed with the first two peaks in Figure 2.17, the remaining three peak frequencies in the range of ω from 0.1 to 200 continue to increase as the value of b_1 increases. Also, at the higher frequencies, more peaks in the curve start to appear for the higher values of b_1. However, most of these peaks are below a transmissibility of 1.0, even below 0.1 in many cases, and are not of much concern because this means the displacement of the bar is much less than the displacement of the base, which is the desired condition for an effective vibration isolator.

The vibration shapes for all five frequency peaks are shown in each figure also. In addition, Figure 2.19 shows vibration shapes for some of the significant valleys of the transmissibility plots. Again, the dark line represents the deflected shape of the model under static equilibrium, and the lighter lines show the vibration of the struts when harmonically excited at the base. Upon observing the peak-frequency vibration shapes for the three different degrees of asymmetry, the behavior of the vibration at each corresponding peak is similar, with a few exceptions. The vibration at the first peak frequency for $b_1 = 0.52$ shows no nodes in the struts, as in the symmetric case. However, the vibration modes of the struts at the initial peak for the higher values of b_1 clearly show a single node. The second peak, which did not occur in the symmetric case, shows the bar pivoting about the equilibrium location and a single node in the struts for all cases of the asymmetric bar. The third peak vibration shape also clearly shows a single node in each case, located at approximately mid-height of each strut, as in the symmetric case. Finally, the fourth and fifth peak vibration shapes are very similar among the symmetric and asymmetric cases studied, showing no nodes in the mode at the fourth peak, and three nodes in the mode at the fifth peak. Therefore, at higher frequencies, the struts seem to be behaving similarly, regardless of the amount of increased static load supported by the right strut.

Because the amplitudes of the horizontal vibration of the struts shown in these figures is sometimes very small in one strut as compared to the other when vibrating at the same frequency, a few of the shapes have been plotted horizontally and increased in scale to show that indeed each strut is vibrating about its equilibrium deflected shape. Figures 2.21, 2.22, and 2.23 are provided at a larger scale than the vibration shapes in the previous figures so that the vibration shape and nodes can be observed in each strut.

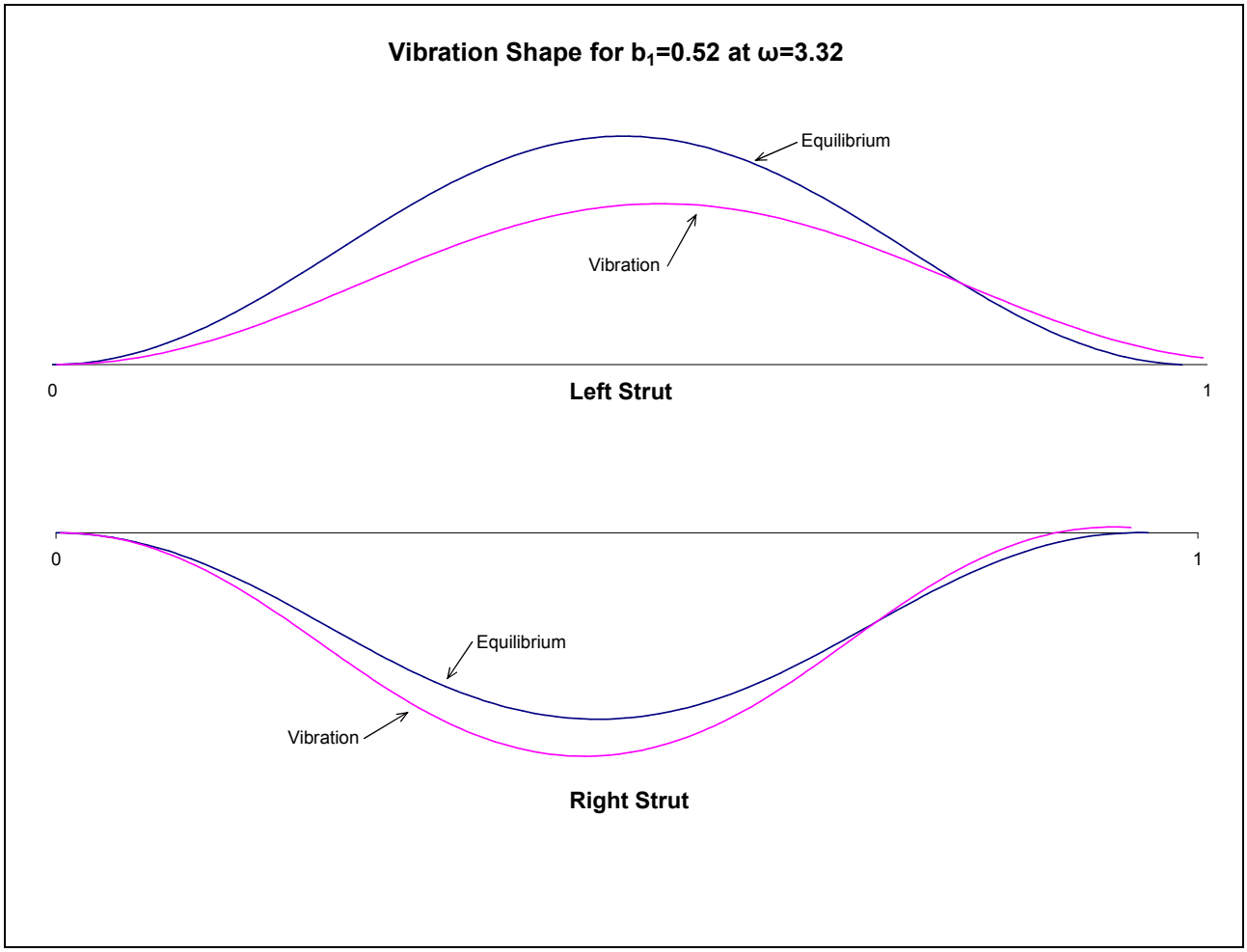

Figure 2.21 Vibration and Equilibrium Shape for Struts of b_1 =0.52 Model at ω = 3.32 (Second Peak Frequency)

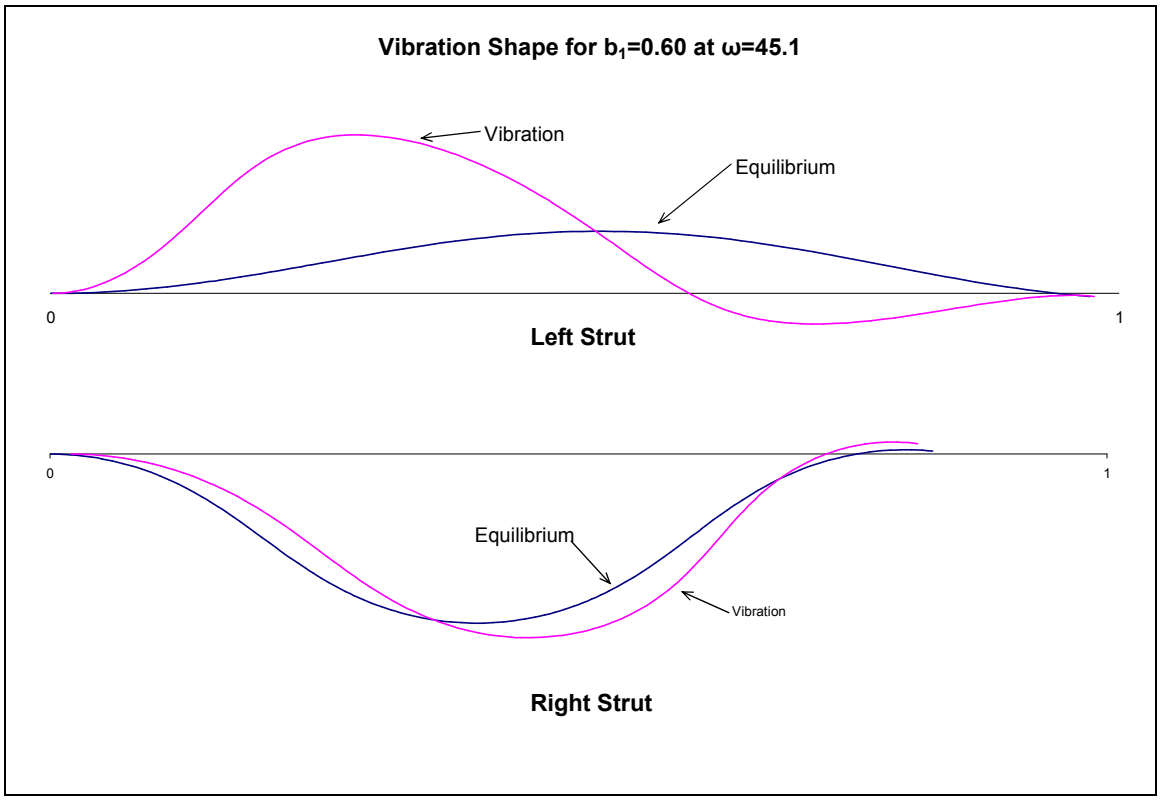

Figure 2.22 Vibration and Equilibrium Shape for Struts of b_1 =0.60 Model at ω = 45.1 (Third Peak Frequency)

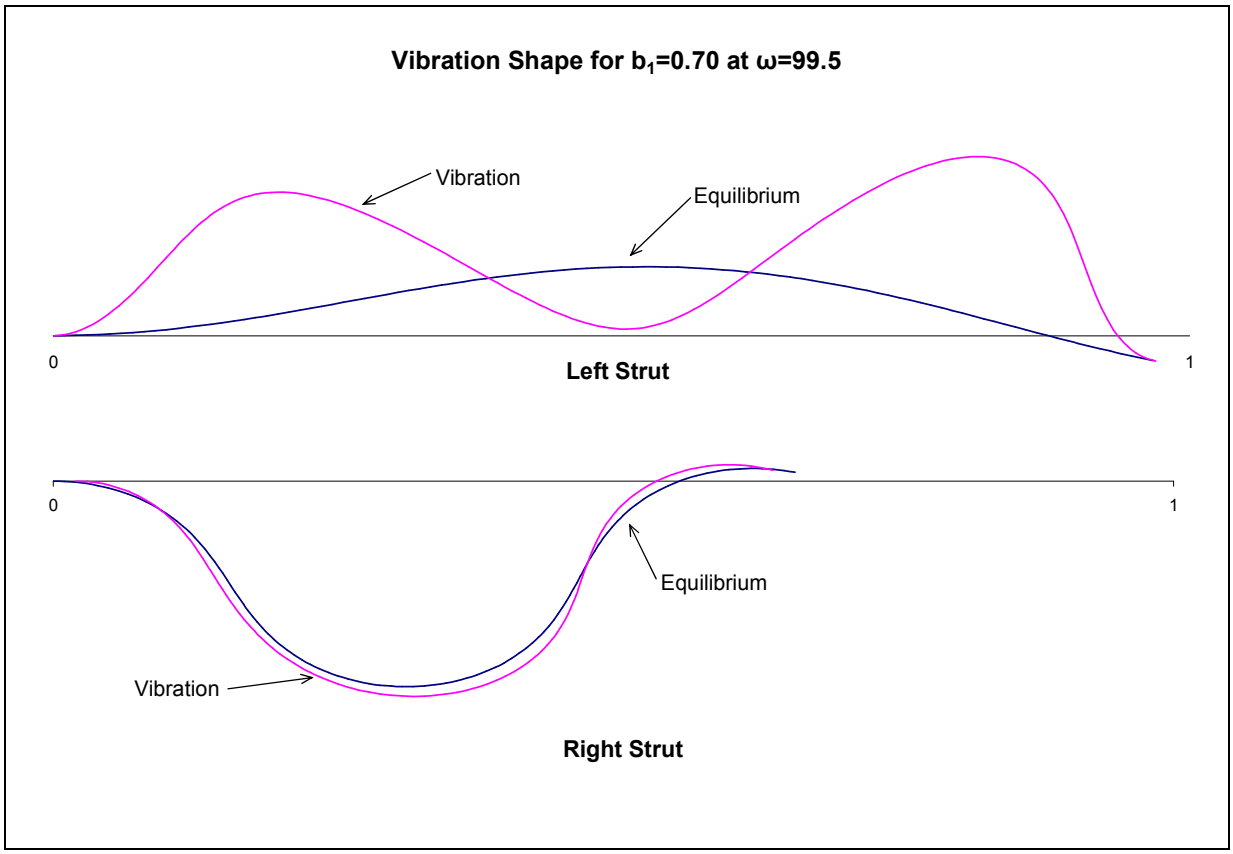

Figure 2.23 Vibration and Equilibrium Shape for Struts of b_1 =0.70 Model at ω = 99.5 (Fourth Peak Frequency)

To further illustrate the increase in each of the frequency peaks for the different values of b_1, the results have been tabulated for comparison in Table 2.2. Each peak frequency that occurred in the range of frequencies studied has been named in order from the lowest, ω_1, to the highest, ω_5.

Table 2.2 Peak Frequencies for Varying Values of b_1

b_1	ω_1	ω_2	ω_3	ω_4	ω_5
0.50	0.697	-	44.7	75.3	173.7
0.52	0.735	3.32	43.8	77.6	176.1
0.55	0.803	3.44	45.0	81.2	176.9
0.60	0.846	3.84	45.1	87.8	178.3
0.65	0.852	4.36	45.2	94.0	180.2
0.70	0.842	4.98	45.7	99.5	182.0

Also, there was a significant "double peak" for ω_3 in the cases of $b_1 = 0.55$ and 0.60, but only one value at each peak is shown in the table. This can also be seen in the transmissibility plots for these two cases, in Figure E.1 and Figure 2.19, respectively. The values in Table 2.2 are also presented graphically in Figures 2.24 – 2.28 to show how each peak frequency varies with the value of b_1.

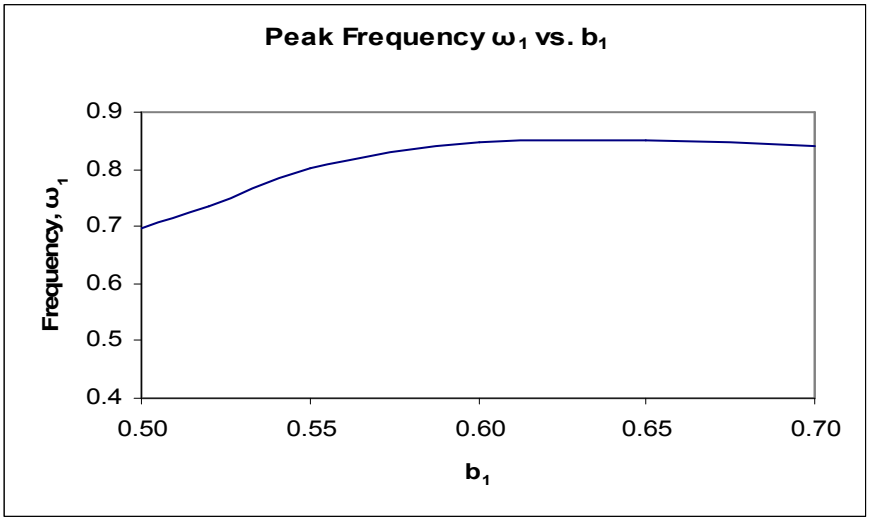

Figure 2.24 Peak Frequency ω_1 vs. b_1

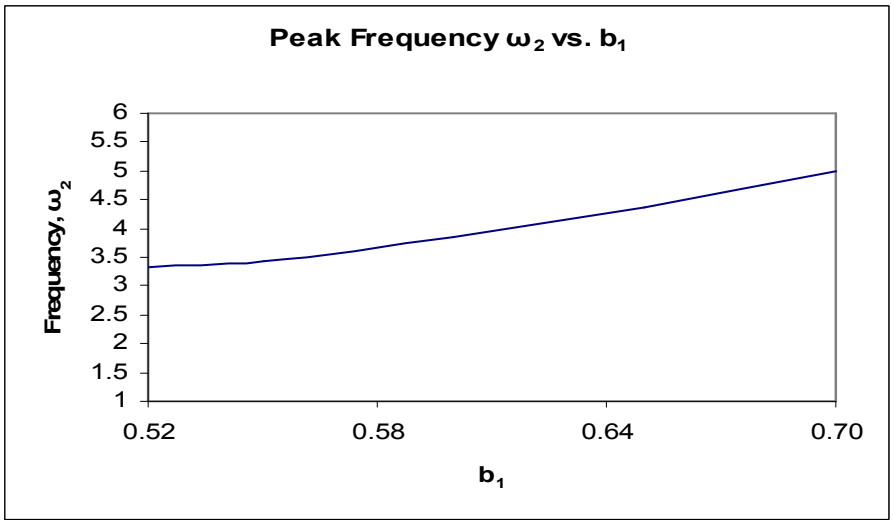

Figure 2.25 Peak Frequency ω_2 vs. b_1

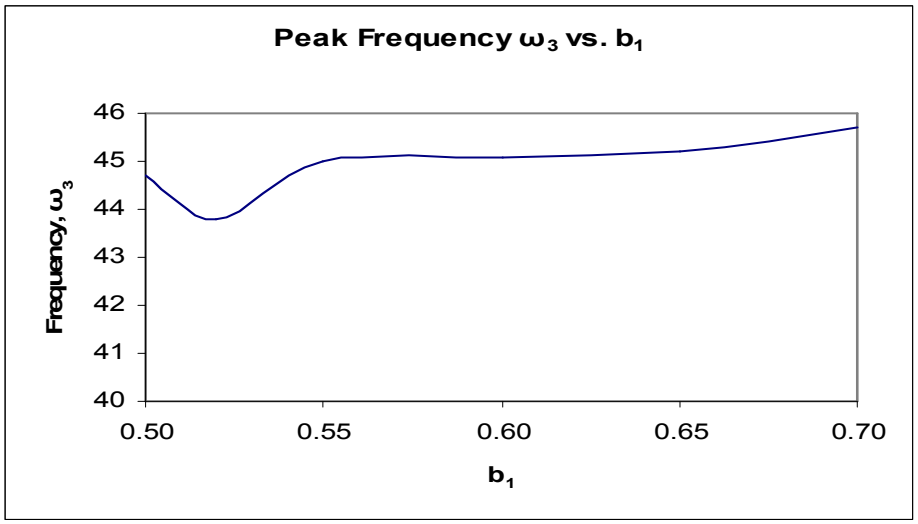

Figure 2.26 Peak Frequency ω_3 vs. b_1

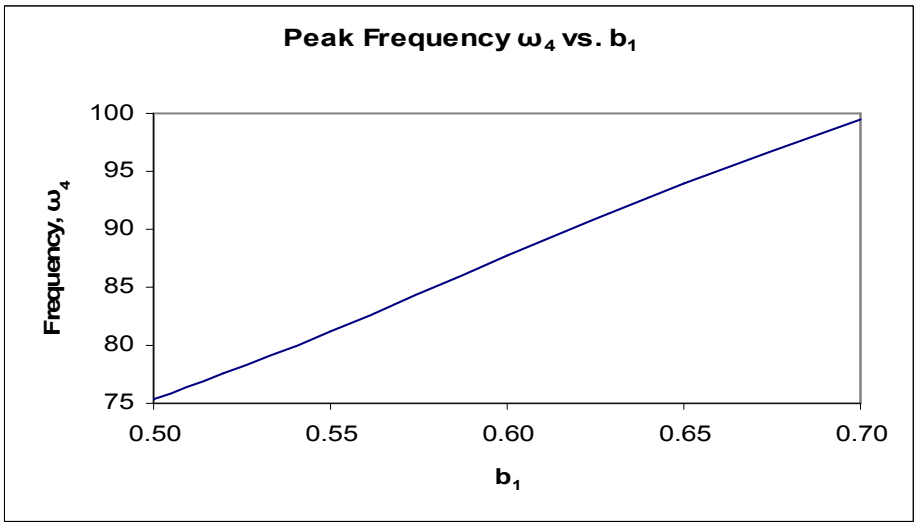

Figure 2.27 Peak Frequency ω_4 vs. b_1

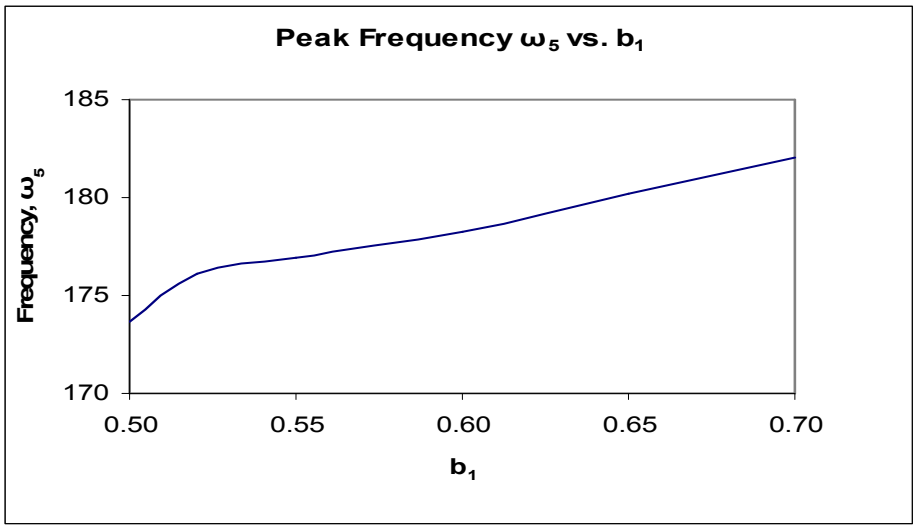

Figure 2.28 Peak Frequency ω_5 vs. b_1

The angle of rotation of the rigid bar relative to the static equilibrium position of the bar, Φ, was also determined for each value of b_1 along the same range of frequencies. The absolute value of the rotation was plotted against the frequency for the same values of b_1, and these plots are presented in Appendix F. The rotation vs. frequency plots are very similar for each value of b_1. In each plot, a sharp valley occurs at nearly the same frequency as the peaks occur in the transmissibility plots, yet there is a peak in the rotational value on either side of this sharp valley. Also, the rotation is minimal in the range of frequencies between the second and third transmissibility peak frequencies, similar to the transmissibility values between these two peaks.

2.4.5 Asymmetric Bar with No Static Rotation

The rotation of the asymmetric rigid bar becomes significantly larger in the equilibrium state as the value of b_1 increases. These exaggerated cases of a large shift in the center of mass of the bar are modeled to study their behavior, but a more likely scenario would be that the bending stiffness EI would be adjusted for each strut to avoid such large static deflections (E being the modulus of elasticity of the strut material and I being the moment of inertia of the cross section of the strut about the axis of bending). By applying a modification factor to the static stiffness of each strut, the right strut can be

strengthened and the left strut weakened so that the bar, although asymmetric, has its bottom edge horizontal in the equilibrium state. However, by modifying the bending stiffness parameter of each strut, the buckling load is no longer a nondimensional load of approximately 40. The modification to the equilibrium and dynamic equations are presented in the following sections. The weight of each strut is assumed to remain the same as before.

2.4.5.1 Equilibrium Analysis Modifications

The modification factor for the right strut is α, and the modification factor for the left strut is β. Therefore, the only variable in the equilibrium analysis that will need to be modified is Equation 2.4, which is rewritten for each strut as follows:

Left strut: $$\frac{d\theta_1}{dS_1} = \frac{M_1}{\beta EI} \tag{2.130}$$

Right strut: $$\frac{d\theta_2}{dS_2} = \frac{M_2}{\alpha EI} \tag{2.131}$$

Therefore, in nondimensional terms, Equations 2.73 and 2.74 are modified as follows:

Left strut: $$\frac{d\theta_1}{ds_1} = \frac{m_1}{\beta} \tag{2.132}$$

Right strut: $$\frac{d\theta_2}{ds_2} = \frac{m_2}{\alpha} \tag{2.133}$$

The modifications to the above equations are made in the equilibrium program, and the program is written with the additional condition that the vertical static displacement of the left strut at $s_1 = 1$ is equal to the vertical static displacement of the right strut at $s_2 = 1$. In other words, another boundary condition is added:

$$x_{1e}(1) = x_{2e}(1)$$

This equation ensures that there is no rotation of the bar under static equilibrium. The program is also modified so that a value of α is given, and the program solves for the corresponding value of β under the new shooting conditions. Values given for α are greater than one, so that the right strut has an increased bending stiffness, and the solution provides a value of β that is less than one.

The buckling load for each strut has now changed so that $p_{cr} = \frac{4\pi^2}{\beta}$ for the left strut and $p_{cr} = \frac{4\pi^2}{\alpha}$ for the right strut. If the initial static load on the model remains the same as in the previous model at $2p_o$, where $p_o = 40$, then the modification factors of α and the corresponding β can be chosen so that the values of p_1 and p_2 obtained from the equilibrium program are just above each strut's corresponding buckling load.

2.4.5.2 Equilibrium Results

The α and the corresponding β that provide a ratio of each strut's p/p_{cr} ratio which is closest in value to the ratio of $\frac{40}{4\pi^2} = 1.013$ are the values that are chosen for the dynamic analysis. Table 2.3 below shows the results of α and the corresponding β that were chosen for each value of b_1 to be subjected to a harmonically forced excitation at the base and analyzed as in the previous section.

Table 2.3 Stiffness Adjustment Factors and Strut Load Ratios

b_1	α	β	p_1/p_{cr1}	p_2/p_{cr2}
0.55	1.09	0.909	1.0138	1.0138
0.60	1.18	0.818	1.0141	1.0141
0.65	1.27	0.728	1.0143	1.0143
0.70	1.36	0.638	1.0144	1.0144

As can be observed from the table, every value of b_1 had α and β values that provided a p/p_{cr} ratio very close to the desired ratio.

2.4.5.3 Dynamic Analysis Modifications

The values of α, β, p_{1e}, p_{2e}, q_{1e}, q_{2e}, m_{1e}, and m_{2e} for each value of b_1 determined from the equilibrium analysis are then used as input for the dynamic analysis program. The equations modified in the dynamic analysis program are Equations 2.93 and 2.94, rewritten as:

Left strut: $$\frac{d\theta_{1d}}{ds_1} = \frac{m_{1d}}{\beta} \tag{2.134}$$

Right strut: $$\frac{d\theta_{2d}}{ds_2} = \frac{m_{2d}}{\alpha} \tag{2.135}$$

2.4.5.4 Dynamic Results

The dynamic analysis program was executed for a range of frequencies from 0.1 to 200 and the transmissibility was determined for each frequency, as before. This was done for b_1 = 0.55, 0.60, 0.65, and 0.70. The results for the first two frequency peaks of each case are plotted, along with the symmetric case for comparison, in Figure 2.29. Upon observing this plot, it is clear that adjusting the strut stiffnesses so that each strut was equally loaded just above their critical buckling load and there was no rotation in the bar at equilibrium did not eliminate the second peak at the low frequency, nor did it eliminate rotation of the bar under the dynamic loading. The rotation vs. frequency plots for the four separate cases of b_1 are provided in Appendix G. When compared to the rotation plots for the asymmetric bar with equal strut stiffnesses (Appendix F), the plots look very similar. The value of the rotation in the adjusted strut stiffness cases is slightly lower, but the shapes of the plots and the location of the peaks and valleys are almost identical. It should be mentioned that the rotation, Φ, in these plots represents the angle of rotation of the bar relative to the static equilibrium position of the bar, not the angle with the horizontal axis. Therefore, even though adjusting the strut stiffnesses eliminated the static rotation of the bottom of the bar, it did not eliminate Φ, the dynamic rotation of the bar about its static equilibrium position.

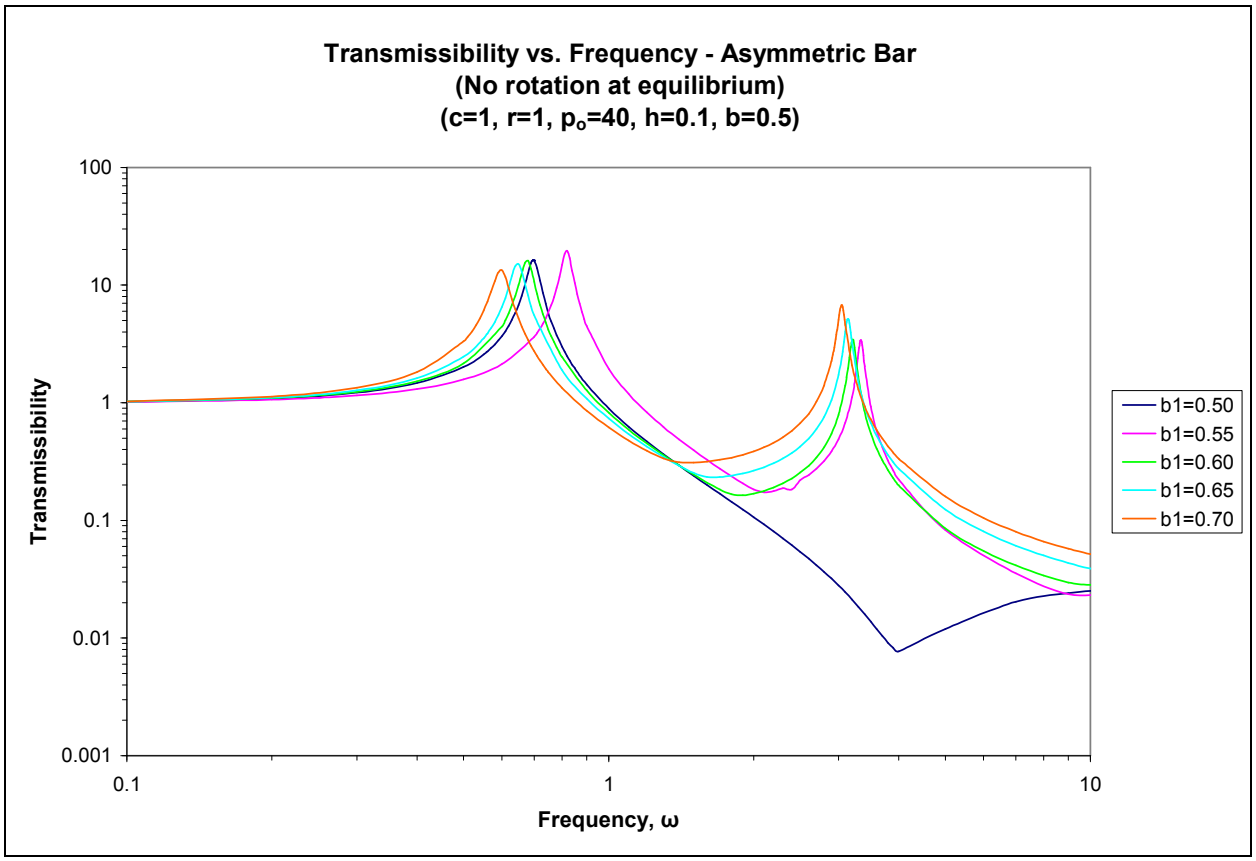

Figure 2.29 Transmissibility vs. Frequency – Adjusted Strut Stiffness for No Rotation at Equilibrium

When comparing the transmissibility plots shown in Figure 2.29, the values of the peak frequencies become lower as the center of mass of the bar shifts farther to the right (i.e., as b_1 increases). This is opposite to the trend found in the asymmetric case when the struts have equal stiffness. Values of all the peak frequencies within the range analyzed are shown in Table 2.4 below. Also note that an additional significant peak in the transmissibility occurred in the range of ω from 81 to ~88.

Table 2.4 Peak Frequencies for Struts with Adjusted Stiffness

b_1	ω_1	ω_2	ω_3	ω_4	ω_5	ω_6
0.50	0.697	-	44.7	75.3	-	173.7
0.55	0.82	3.34	42.4	72.2	81	165
0.60	0.68	3.2	40.2	68.6	81.8	160
0.65	0.65	3.14	38	64.8	84.8	148
0.70	0.6	3.05	35.6	60.8	87.6	141

Graphical representations of the data in Table 2.4 are shown in Appendix G to further illustrate the change in peak frequencies for different values of b_1.

In order to compare the transmissibilities of the two cases, the asymmetric bar with equal strut stiffness vs. adjusted strut stiffness, they are plotted on the same graph for each of the four values of b_1 being studied. This is shown in Figures 2.30-2.33. The dark line in each figure represents the case of equal strut stiffness (the case presented in Section 2.4.5) and the lighter line represents the adjusted strut stiffness case. For each of the values of b_1, the values of the peak frequencies are lower for the adjusted strut stiffness, and the more asymmetric the bar, the larger the gap between the two peaks. Also, the valleys are more pronounced in the equal strut stiffness cases, particularly at the higher values of b_1. However, the overall value of the transmissibility of the adjusted strut stiffness model tends to be lower.

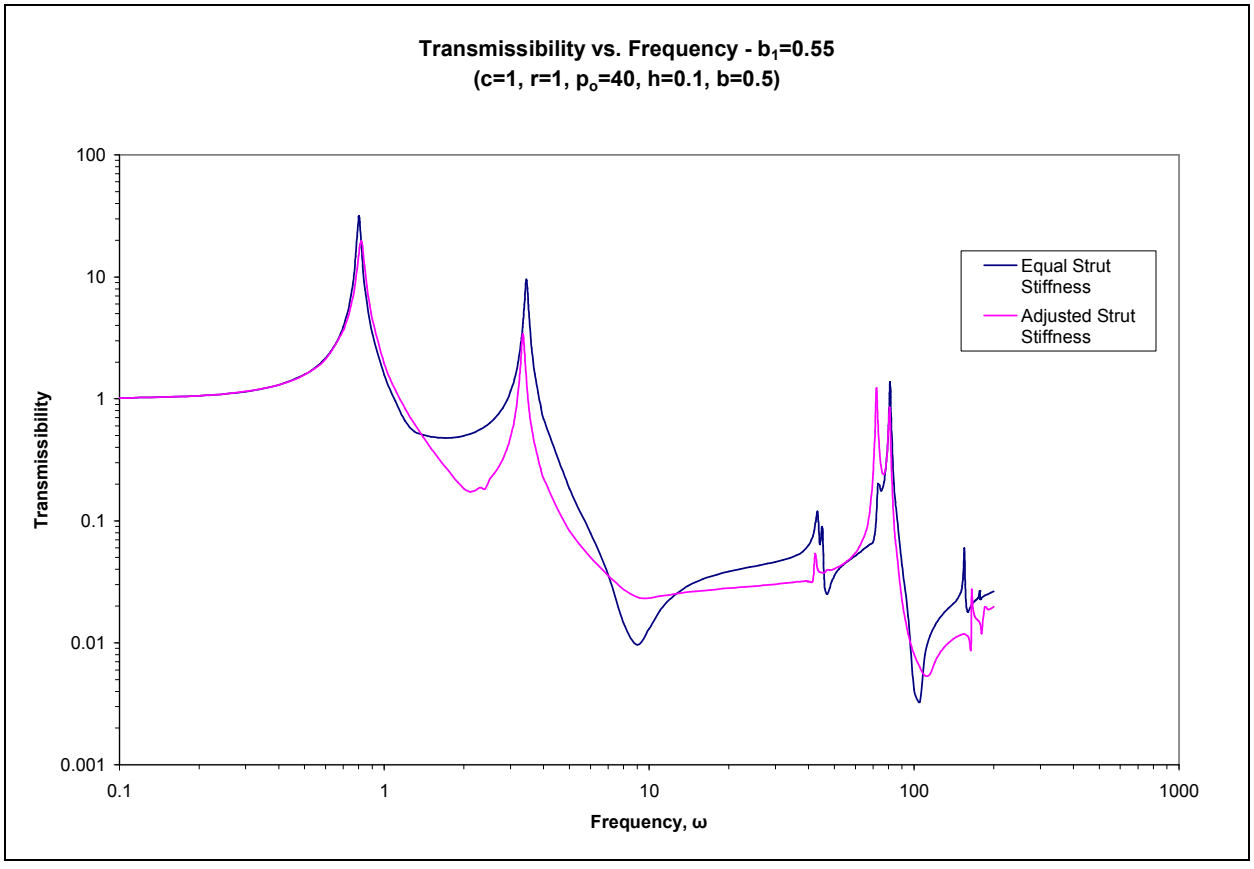

Figure 2.30 Transmissibility vs. Frequency for Two Cases of $b_1 = 0.55$

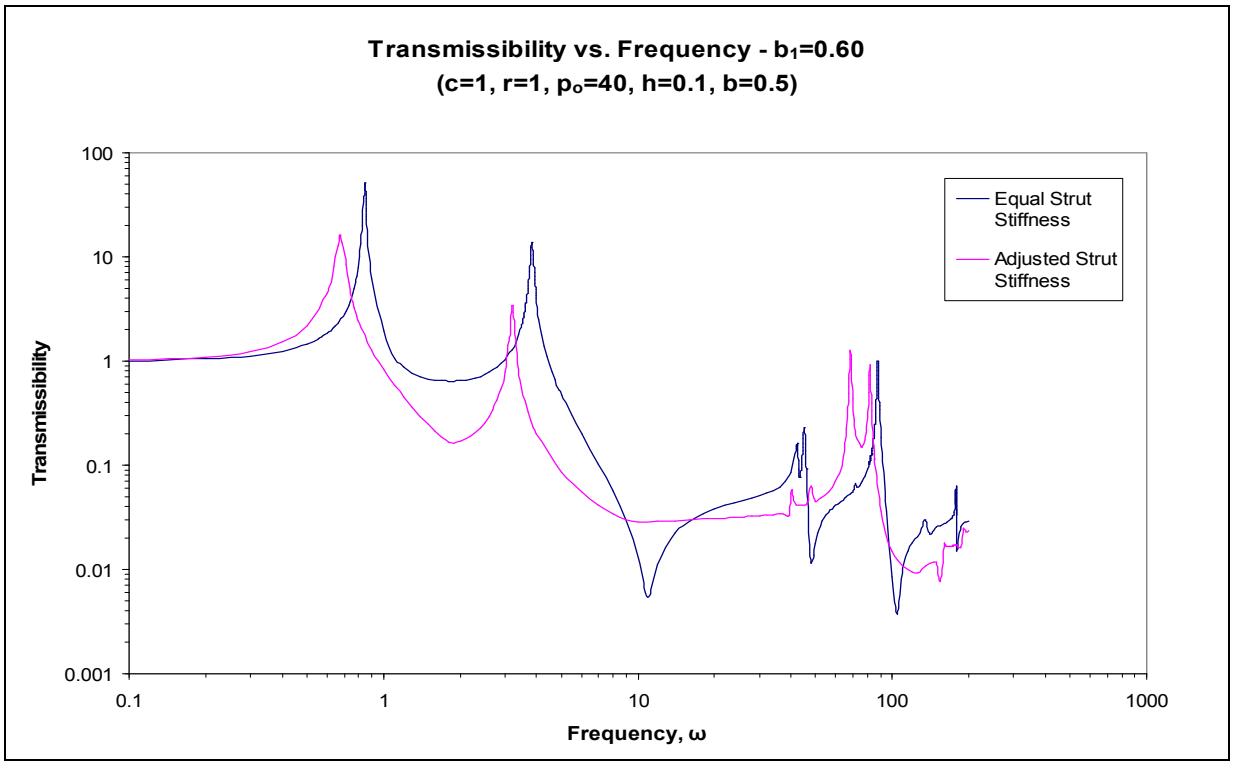

Figure 2.31 Transmissibility vs. Frequency for Two Cases of $b_1 = 0.60$

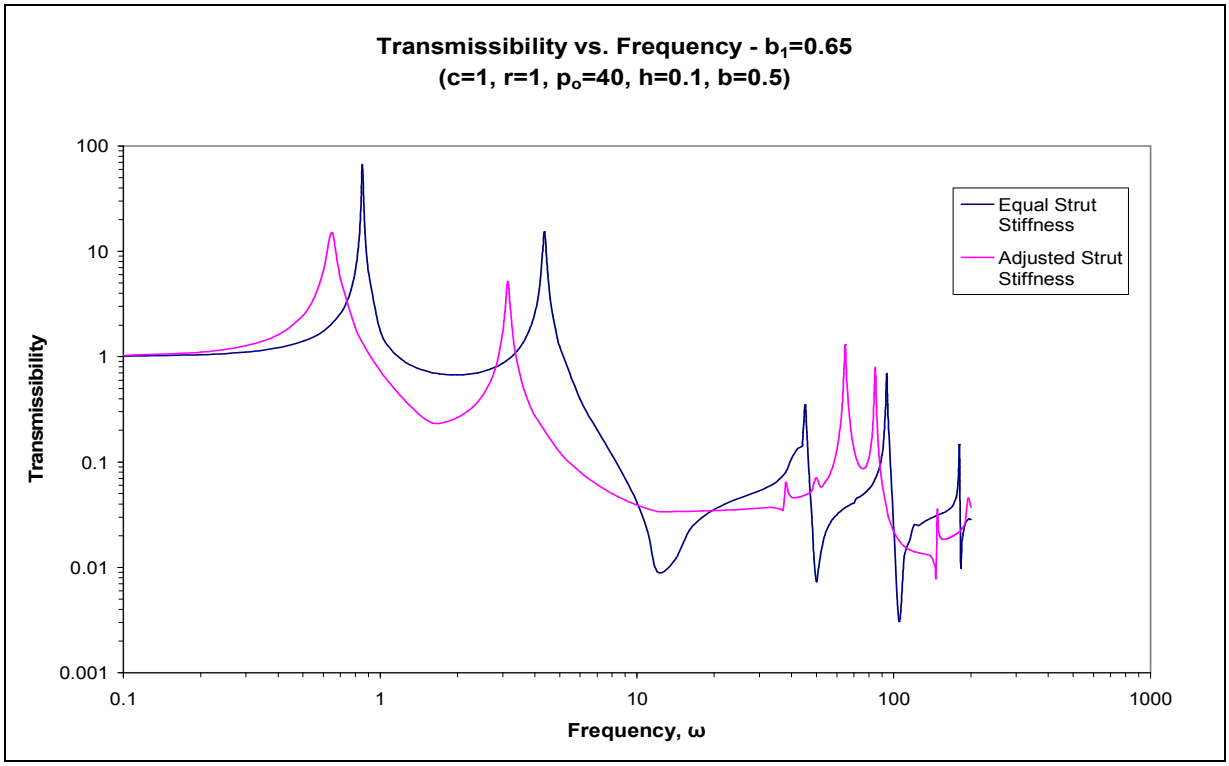

Figure 2.32 Transmissibility vs. Frequency for Two Cases of $b_1 = 0.65$

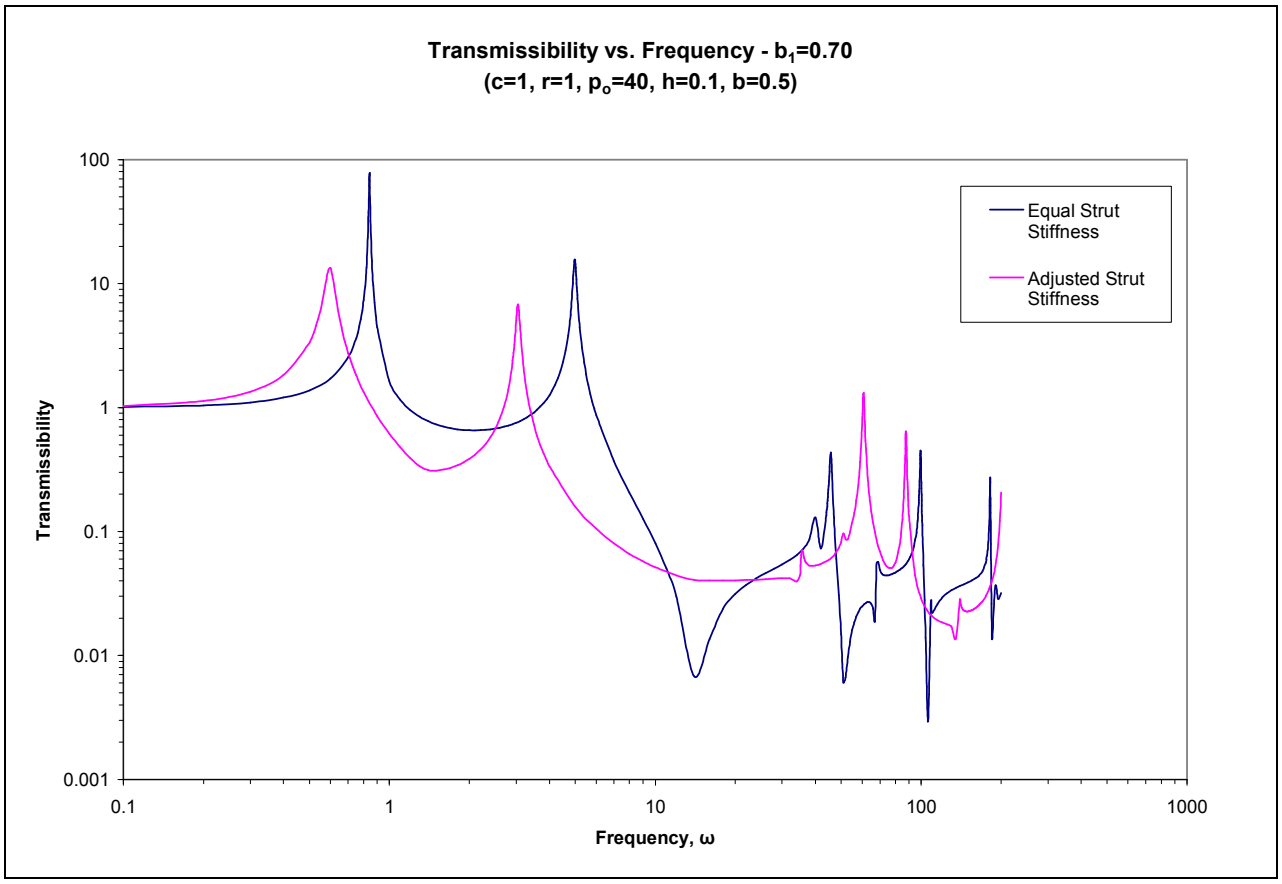

Figure 2.33 Transmissibility vs. Frequency for Two Cases of $b_1 = 0.70$

Vibration shapes of the adjusted strut stiffness models for values of $b_1 = 0.60$ and $b_1 = 0.70$ were also generated for comparison with the equal strut stiffness vibration shapes. These shapes can be found in Appendix G. These vibration shapes look very similar to those for the symmetric bar case. The location and number of nodes of the vibration shapes at the different peak frequencies are the same for the vibration shapes of the symmetric bar and the asymmetric bar with equal strut stiffness models.

2.5 Summary and Conclusions

Two basic models have been presented in this chapter, along with a slight variation in the second model. The first model is the ideal case of two equal struts supporting a rigid bar with a center of mass at its geometric center. The load of the bar is such that the struts are equally loaded just above their buckling load. The second model is different from the

first in that the bar is asymmetric in mass, thus loading each strut differently. But because the struts are equal, only one strut (the right strut in the model) is loaded above its buckling load. Lastly, the second model is modified by introducing an adjustment factor to each strut's bending stiffness so that the bottom of the asymmetric bar is supported in a horizontal position in the equilibrium state. Hence each strut is loaded just above its buckling load as in the first model, but the static loads are different.

By examining the results of each model described, several conclusions can be drawn. First, it is apparent that the behavior of the ideal case of the first model presents the best situation for utilizing post-buckled struts as vibration isolators. It is the only model that produces a single peak in the transmissibility plot at a low frequency. Therefore, it provides the widest range of frequencies at which the transmissibility is well below unity, which is the goal of the vibration isolator. It was also found that the direction of the horizontal deflection of the buckled struts, whether towards each other or away, had no effect on the transmissibility results. However, when analyzing the asymmetric bar case, it was determined that outward buckling of the struts was the most stable condition.

In all cases studied, when asymmetry of the supported load was introduced, a second peak at low frequencies was observed. This suggests that the second peak is caused by the offset of the center of mass and not the difference in the ratio of each strut's load to its buckling load. It was also learned by examining the asymmetric case with equal strut stiffnesses that even though the left strut in all cases was loaded *below* its buckling load, the system still produced approximately the same range of frequencies for which the transmissibility was below unity as in the case in which both struts were in the post-buckled state, given the same amount of asymmetry to the supported load. Therefore, the advantage obtained by adjusting the stiffness of each strut so that they are both loaded slightly above their buckling load is that the bottom of the bar is horizontal; no noticeable improvement is noted when comparing the transmissibility plots.